Ascending dorsal column sensory neurons respond to spinal cord injury and downregulate genes related to lipid metabolism

Eric E. Ewan[1], Dan Carlin[1], Tassia Mangetti Goncalves[1], Guoyan Zhao[1], and Valeria Cavalli[1,2,3*]

1. Department of Neuroscience, Washington University School of Medicine, St Louis 63110, Missouri, USA

2. Hope Center for Neurological Disorders, Washington University School of Medicine, St. Louis, Missouri 63110, USA

3. Center of Regenerative Medicine, Washington University School of Medicine, St. Louis, Missouri 63110, USA

*Correspondence to: Valeria Cavalli, Department of Neuroscience, Washington University School of Medicine, Campus Box 8108, 660 S. Euclid Ave, St. Louis, MO 63110-1093 Phone: 314 362 3540, Fax: 314 362 3446, E-mail: cavalli@wustl.edu

Abstract

Regeneration failure after spinal cord injury (SCI) results in part from the lack of a pro-regenerative response in injured neurons, but the response to SCI has not been examined specifically in injured sensory neurons. Using RNA sequencing of dorsal root ganglion, we determined that thoracic SCI elicits a transcriptional response distinct from sciatic nerve injury (SNI). Both SNI and SCI induced upregulation of ATF3 and Jun, yet this response failed to promote growth in sensory neurons after SCI. RNA sequencing of purified sensory neurons one and three days after injury revealed that unlike SNI, the SCI response is not sustained. Analysis of differentially expressed genes revealed that lipid biosynthetic pathways, including fatty acid biosynthesis, were differentially regulated after SCI and SNI. Pharmacologic inhibition of fatty acid synthase, the enzyme generating fatty acid, decreased axon growth *in vitro*. These findings suggest that decreased fatty acid synthesis inhibits axon regeneration after SCI.

Introduction

Unlike injured neurons in the peripheral nervous system, which mount a regenerative response and reconnect with their targets, axon regeneration typically fails after spinal cord injury (SCI). In addition to the growth inhibitory environment of the injured spinal cord (Sofroniew, 2018; Tran, Warren, & Silver, 2018), gene profiling studies link regenerative failure after SCI to the lack of an intrinsic transcriptional response (Kadoya et al., 2009; Palmisano et al., 2019). This is supported by the conditioning injury paradigm, in which prior injury to the peripheral axons of dorsal root ganglion (DRG) sensory neurons promotes axon regeneration of their central axons after SCI (McQuarrie & Grafstein, 1973; Neumann & Woolf, 1999; Richardson & Issa, 1984). Peripheral nerve injury upregulates many regeneration-associated transcription factors (RATF) (Blackmore, 2012; Mahar & Cavalli, 2018), yet only modest spinal axon regeneration has been observed by overexpressing RATF (Blackmore et al., 2012; Gao et al., 2004; Z. Wang, Reynolds, Kirry, Nienhaus, & Blackmore, 2015). This suggests that RATF expression does not sufficiently recapitulate a growth program and that the intrinsic mechanisms underlying regeneration failure after SCI remains incompletely understood.

Whether and how sensory neurons alter their transcriptome after SCI remains unclear because most analyses have used whole DRG after SCI (Kadoya et al., 2009; Loh et al., 2017; Palmisano et al., 2019), which includes uninjured nociceptors (Yasko, Moss, & Mains, 2019) and non-neuronal cells (Thakur et al., 2014). In this study, we took advantage of a mouse line that labels sensory neurons ascending the spinal cord, dorsal column (DC) neurons, to unravel their transcriptional response to SCI. We performed RNA sequencing (RNA-seq) experiments from whole DRG and fluorescence-activated cell sorted (FACS) DC neurons acutely after SCI and SNI. Our results indicate that DC neurons alter their transcriptome after SCI, with gene expression changes that differ from SNI. The transcriptional changes observed after SCI, which are related to defects in lipid metabolism, may repress axon regeneration.

Results and Discussion

SCI induces a unique transcriptional response in the DRG compared with PNS injury.

Previous studies suggest that transcriptional changes in whole DRG after SCI may occur early after SCI and might not be sustained (Kadoya et al., 2009; Palmisano et al., 2019). SNI was shown to induce a more robust transcriptional response compared to SCI in whole DRG (Palmisano et al., 2019). In contrast, SCI induces more changes in 5-hydroxymethylcytosine (5hmC) than SNI, an epigenomic mark that has transcriptional regulatory roles (Loh et al., 2017). To better understand the transcriptional response in DRG after SCI and SNI, we performed RNA-seq of L4 DRG one day (1d) after SCI and analyzed our results with a previously generated RNA-seq data set collected 1d after SNI (**Fig 1A**; (J. E. Shin, Ha, Kim, Cho, & DiAntonio, 2019)). We found that SCI elicits a less robust transcriptional response in the DRG compared to SNI, with fewer differentially expressed (DE) genes compared to SNI (**Fig 1B**). There were few DE genes overlapping between conditions (~15%) and many (~9%) were inversely expressed (**Fig 1B**). KEGG (Kyoto Encyclopedia of Genes and Genomes biological) pathway analysis of DE genes identified different pathways enriched after SNI and SCI (**Fig S1A-B**), suggesting that the SCI response is distinct from the SNI response.

We next examined the expression of RATFs, given their important roles in establishing a regenerative axon growth program (Fagoe, van Heest, & Verhaagen, 2014; Mahar & Cavalli, 2018). Whereas all RATFs examined were upregulated after SNI, only ATF3 and Jun were increased after SCI (**Fig 1C**). The activation of RATFs is believed to arise in part from retrograde transport of kinases from the injury site back to the cell soma (Abe & Cavalli, 2008; Rishal & Fainzilber, 2014). The dual leucine zipper kinase DLK is required for retrograde injury signaling and induction of RATF after nerve injury (J. Shin et al., 2012; J. E. Shin et al., 2019), and is significantly decreased after SCI (0.29 fold, p-adj < 0.05). To determine if the limited transcriptional upregulation of RATF's after SCI relates to decreased levels of DLK, we used previously generated RNA-seq data that examined the transcriptional response to nerve injury in

mice lacking DLK (DLK KO; (J. E. Shin et al., 2019)). Comparison of DE genes and KEGG pathway analysis in DLK KO following SNI and wildtype mice following SCI revealed little overlap between conditions (**Fig S1B-D**), suggesting that the diminished RATF upregulation after SCI is unlikely mediated by reduced DLK signaling.

The unique transcriptional response of SCI in the DRG compared to SNI may result in gene expression that actively represses axon regeneration after SCI. To examine this possibility further, we performed KEGG pathway analysis on DE genes that were inversely expressed between conditions. We found inversely expressed DE genes were associated with biosynthetic and lipid metabolic pathways (**Fig 1D-H**). These pathways were also some of the most downregulated by SCI when all DE genes were examined (**Fig S1B**). This is particularly interesting since previous studies using DRG cultures revealed that synthesis of phosphatidylcholine and cholesterol is required for axonal growth (Posse de Chaves, Vance, Campenot, & Vance, 1995; Vance, Campenot, & Vance, 2000; Vance, Pan, Campenot, Bussiere, & Vance, 1994). Furthermore, in the optic nerve injury model it was shown that increasing phospholipid synthesis and decreasing triglyceride synthesis promotes axon regeneration (Yang et al., 2020). Together, these results suggest that defects in lipid synthesis may restrict axon regeneration after SCI.

ATF3 and Jun upregulation after SCI is not sufficient to promote growth *in vitro*.

ATF3 and Jun are necessary for peripheral nerve regeneration (Raivich et al., 2004). When co-expressed in cultured DRG neurons, ATF3 and Jun promote axon growth *in vitro* (Chandran et al., 2016) and regeneration of the central axon branch of sensory neurons *in vivo* (Fagoe, Attwell, Kouwenhoven, Verhaagen, & Mason, 2015). We thus determined if ATF3 and Jun upregulation after SCI occurs in DC neurons. We used Thy1-YFP16 mice (Feng et al., 2000), which label large diameter DC neurons (Di Maio et al., 2011; Taylor-Clark et al., 2015). These DC

neurons ascend the spinal cord and are injured by thoracic SCI (Niu et al., 2013) (**Fig 2A**). DC neurons are distinct from nociceptors in that they express NF200 (NEFH) but not TrkA (Usoskin et al., 2015) and we confirmed that YFP neurons were NF200 positive and TrkA negative (>90%, **Fig 2B-C**). We found that after SNI, ATF3 and Jun were expressed in nearly two-thirds of all DRG neurons, with equal numbers between YFP positive and negative neurons (**Fig 2D-E; Fig S2A-B**). In contrast, only ~5% of all DRG neurons expressed ATF3 and Jun after SCI, but ~20% of YFP neurons were ATF3 and Jun positive (**Fig 2D-E; Fig S2A-B**). We next asked whether this increased ATF3 and Jun expression in YFP neurons promotes axon growth *in vitro* 3 days after SCI. We observed that unlike SNI, SCI failed to induce a conditioning effect *in vitro* in YFP neurons compared to naive (**Fig 2F-G).** These results suggest that the other transcriptional changes elicited by SCI we observed (Fig 1D-H) may repress the pro-growth effects associated with ATF3 and Jun expression. It is also possible that ATF3 and Jun need to be expressed in the same cells to synergize (Chandran et al., 2016); we think this is likely, but limitations with antibodies did not permit us to confirm co-expression of ATF3 and Jun in injured DC neurons.

SCI induces a unique transcriptional response in DC neurons compared to SNI.

Neurons are outnumbered by non-neuronal cells at least 10-fold in DRG (Thakur et al., 2014). Furthermore, not all lumbar DRG neurons project to the spinal cord and are injured by T9 SCI (Niu et al., 2013). Thus, to define the transcriptional changes elicited by SCI in DC neurons specifically, we performed RNAseq 1 and 3 days after SCI or SNI in FACS-sorted DC neurons from YFP16 mice (**Fig 3A**). This approach allowed us to enrich for DC neurons, based on the expression levels of known neuronal marker genes (Usoskin et al., 2015) when comparing FACS-sorted and whole DRG samples (**Fig 3B**). We found that SCI elicited fewer DE genes compared to SNI at 1d and 3d (**Fig 3C-D**). There was little overlap between the two conditions, with only ~37% for upregulated genes and ~23% for downregulated genes (**Fig 3C)**. Whereas the numbers of DE genes were increased from 1 to 3 days after SNI, DE genes decreased from 1 to 3 days

after SCI (**Fig 3D**), suggesting that the SCI response is not sustained over time. This may explain why few transcriptional changes in whole DRG were observed 7 days after SCI (Kadoya et al., 2009). Why transcriptional responses would decrease in time after SCI is unclear, but one possibility is inhibitory signaling from newly established CSPG's at the injury site, which can be observed as early as 1dpi (Jones, Margolis, & Tuszynski, 2003). Another possibility is anatomical, since SCI leaves the peripheral sensory branch intact. Therefore, the continuous sensory input form the peripheral branch may restrict the expression of an injury response. This is consistent with the notion that electrical activity suppresses axon growth and limits regenerative ability in the injured CNS (Enes et al., 2010; Tedeschi et al., 2016; Tedeschi & He, 2010).

We next examined the expression of RATF known to promote axon growth (Fagoe et al., 2014; Mahar & Cavalli, 2018). We found that all assessed RATFs were upregulated in DC neurons 1 and 3 days after SNI (**Fig 3E**). In contrast, only ATF3 and Smad1 were increased 1 and 3 days after SCI. KLF6 and Creb1 expression increased at 1d, while Sox11 increased at 3d after SCI (**Fig 3E**). The SNI-induced upregulation of RATFs in DC neurons was remarkably similar to the response we previously reported in FACS-sorted nociceptors (**Fig S3A-B**) (Carlin, Halevi, Ewan, Moore, & Cavalli, 2019). This is consistent with recent findings indicating that after peripheral nerve injury most sensory neurons adopt a similar transcriptomic state (Nguyen, Le Pichon, & Ryba, 2019). The unique effects of SCI on DC neurons are thus unlikely related to any intrinsic transcriptional differences between sensory neuron subtypes within the DRG.

To better understand the transcriptional differences in DC neurons after SNI and SCI, we performed KEGG pathway analysis of DE genes. We identified very different pathways activated after SCI and SNI (**Fig S3C-F**), with the 5 most enriched KEGG pathways associated with biosynthetic and lipid metabolic pathways 1d after SCI (**Fig S3D**). The top 3 downregulated biosynthesis pathways 1d after SCI were steroid biosynthesis, fatty acid biosynthesis, and terpenoid backbone biosynthesis, all of which were also identified in whole DRG analysis 1d after SCI (**Fig S1B**). None of these pathways were downregulated by SNI, and instead steroid

biosynthesis was upregulated both 1d and 3d after SNI (**Fig S3C,E**). Further analysis of the genes in these pathways indicated that most genes were more significantly downregulated after SCI, than SNI, and some were upregulated by SNI (**Fig 3F**). These results reveal that biosynthetic and lipid metabolic pathways are downregulated specifically in DC neurons after SCI, and may repress axon regeneration.

The FACSeq analysis detected fewer DE genes for both SNI and SCI compared to whole DRG RNA-seq. Differences in methodology may underlie these results, since dissociation and FACS sorting induces an acute axon injury in DRG neurons and sorting 100 YFP+ neurons in triplicate introduces added variability due to random sampling. Nonetheless, our analysis revealed many DE genes (>500) in DC neurons, which is significantly more than that observed (<100) in FACS-sorted nociceptors after compression SCI (Yasko et al., 2019), which are not directly injured by SCI (Niu et al., 2013). Furthermore, we found that only 43% and ~13% of DE genes identified in FACS-sorted DC neurons after SNI and SCI, respectively, overlapped with DE genes identified from whole DRG (**Fig S3G S3H**). Many genes are likely not identified in whole DRG because unlike SNI, SCI only directly injures the DC neurons subpopulation within the DRG.

Fatty acid synthase (Fasn) inhibition decreases DRG axon growth *in vitro*.

Fasn is an enzyme responsible for *de novo* fatty acid synthesis (Dean & Lodhi, 2018) and is one of the genes downregulated in DC neurons after SCI (**Fig 3F**). Fasn synthesizes palmitic acid, which is the substrate for the synthesis of more complex lipids including phospholipids (Dean & Lodhi, 2018). Given the role of phospholipids synthesis in axon growth (Posse de Chaves et al., 1995; Vance, De Chaves, Campenot, & Vance, 1995; Vance et al., 1994), we assessed the potential role of Fasn in axon growth by testing whether inhibiting fatty acid synthesis impairs axon growth. Cultured DRG neurons treated with the Fasn inhibitor platensimycin, which was shown to effectively inhibit fatty acid synthesis *in vitro* (Wu et al., 2011), displayed ~40% decrease in axon growth after 24hr in culture (**Fig 4A-B**). This supports the notion that decreased lipid

metabolism-related genes after SCI, including Fasn, may repress axon regeneration after SCI. Since our adult cultures include both neurons and non-neuronal cells, we cannot rule out a potential role for Fasn inhibition on non-neuronal cells in decreasing axon growth *in vitro*. Indeed, neurite growth in culture hippocampal neurons was shown to be supported by phospholipid loaded lipoproteins secreted from glial cells (Nakato et al., 2015).

Fasn serves as a primary source of endogenous palmitate, which is critical for protein palmitoylation (Wakil, Stoops, & Joshi, 1983). Both Gap43 and SCG10 proteins are palmitoylated and anterogradely transported after nerve injury (Holland & Thomas, 2017). Palmitoylation of SCG10 facilitates its targeting to the growth cone (Di Paolo et al., 1997; Lutjens et al., 2000) and axonal transport of SCG10 has widely been used to label regenerating axons (J. E. Shin, Geisler, & DiAntonio, 2014). We found that SNI, but not SCI, induces upregulation of Gap43 and SCG10 (**Fig S4A-B**). We next tested if SGC10 accumulation fails to occur in injured DC axons after SCI. We performed a unilateral conditioning SNI, followed by thoracic SCI along with tracer injection into the conditioned sciatic nerve 3 days later, and histology assessment of the DC 1d later (**Fig S4C**). Since the tracer labels only ipsilateral dorsal column axons, we can assess both conditioned (ipsilateral, tracer-labeled) and unconditioned (contralateral, unlabeled) axons in the same animal and tissue section. We found that SCG10 accumulates in injured spinal axons of ascending DC neurons only after a conditioning injury (**Fig 4C**). This is consistent with previous findings showing that CNS axons increase axonal transport after peripheral conditioning (Mar et al., 2014). SCG10 accumulation in PNS axon tips is associated with neurite growth and regeneration (Morii, Shiraishi-Yamaguchi, & Mori, 2006; Riederer et al., 1997; J. Shin et al., 2012), whereas SCG10 degradation has surprisingly been suggested to promote axon growth after SCI (He et al., 2016). Our results suggest that axonal transport of SCG10 fails to occur in the CNS, which may be partially mediated through diminished protein palmitoylation as a consequence of decreased Fasn levels. This is consistent with the notion that decline of intrinsic axon regenerative ability is associated with selective exclusion of key molecules from CNS axons, and that

manipulation of transport can enhance regeneration (Koseki et al., 2017). Fasn is also thought to facilitate membrane outgrowth (Zhang, Lu, Su, Yang, & Zhou, 2017), in part by cooperating with protrudin, which is known to induce neurite formation (Shirane & Nakayama, 2006). These results indicate that Fasn inhibition may impact neural growth at multiple levels. Whether Fasn expression can increase axon growth after SCI remains to be tested.

Conclusion

Our results reveal that DC neurons respond to SCI and alter their transcriptome in a way that differs from SNI. The upregulation of stress response genes such as ATF3 and Jun suggest that DC neurons can sense injury after SCI and mount a stress response, but this response is not sufficient to promote a growth state. This suggests that other mechanisms may inhibit DC neuron growth. We identified downregulation of lipid biosynthesis related genes in DC neurons after SCI as one possible mechanism that inhibits DC neuron growth. Pharmacologic inhibition of the enzyme generating fatty acid, Fasn, decreases axon growth *in vitro*. These results are consistent with the notion that phospholipid synthesis is required for axon growth in cultured neurons (Posse de Chaves et al., 1995; Vance et al., 1995; Vance et al., 1994) and *in vivo* in retinal ganglion cells (Yang et al., 2020).

Materials & Methods

Animals & Surgical Procedures

All procedures were performed according to approved guidelines by the Washington University in St. Louis School of Medicine Institutional Animal Care and Use Committee. Adult female mice (C57/Bl6, Envigo; Thy1-YFP16, Jackson; 10-20 weeks) were used due to ease of bladder voiding after SCI. Buprenorphine SR-LAB (1mg/kg, subcutaneous, ZooPharm) was administered 1 hour before surgery for analgesia. During surgery mice were anesthetized with 2.5% isoflurane. Surgical sites were shaved and disinfected with povidone-iodine solution (Ricca)

and alcohol. After surgery underlying tissue was sutured with absorbable sutures and the skin closed with wound clips.

For sciatic nerve injury (SNI), a small skin incision (~1cm) was made at midthigh, the underlying tissue separated by blunt dissection, and the right sciatic nerve exposed and crushed with fine forceps for 5 seconds. For tracer injection into the sciatic nerve, 2ul of 10% dextran, texas red (Thermo Fisher, Cat # D-3328) was injected using a 5ul Hamilton syringe. For spinal cord injury (SCI), a small midline skin incision (~1cm) was made over the thoracic vertebrae at T9−T10, the paraspinal muscles freed, and the vertebral column stabilized with metal clamps placed under the T9/10 transverse processes. Dorsal laminectomy at T9/10 was performed with laminectomy forceps, the dura removed with fine forceps, and the dorsal column transversely cut using fine iridectomy scissors.

Tissue Processing & Immunohistochemistry

Immediately after euthanasia mice were transcardially perfused with 10mL of PBS followed by 10mL of 4% paraformaldehyde (PFA) in PBS (FD Neurotechnologies; PF101). Tissue was dissected and post-fixed in 4% PFA for 4 hours and then cryoprotected in 30% sucrose overnight. All tissue was sectioned using a cryostat at 10um except for spinal tissue (20um). For immunohistochemistry, tissue sections were blocked in 5% donkey serum in 0.2% PBST (1hr) and incubated overnight at 4°C in primary antibodies diluted in the blocking solution. The next day sections were incubated in secondary antibodies (1:500; 1hr) in PBS and coverslipped in ProLong Gold antifade mounting media (Thermo Fisher). Between steps tissue sections were washed with PBS. For image acquisition, a Nikon TE-2000E microscope equipped with a Prior ProScan3 motorized stage was used. Nikon Elements software was used for image analysis.

Cell Culture

Immediately after euthanasia mice were transcardially perfused with 10mL of Hanks'

balanced salt solution with 10 mM HEPES (HBSS-H) and L4 DRG dissected into HBSS-H on ice. DRG were treated with papain (15 U/ml, Worthington Biochemical) and collagenase (1.5 mg/ml, Sigma-Aldrich) in HBSS-H at 37C for 20 minutes, then dissociated by trituration into 3 or 4 wells of a 24-well glass-bottom plate coated with 100 ug/ml poly-D-lysine and 3 ug/ml laminin. Culture media consisted of Neurobasal-A medium, B27 plus, glutaMAX, and penicillin/streptomycin. For experiments assessing Fasn inhibition, vehicle (0.05% DMSO) or platensimycin (1um) was added to the media 30 minutes after plating. After 24hr cells were fixed with 4% PFA for 20 minutes and then immunostained as described above.

Image Analysis

Total neurons were identified using TUJ1 (BioLegend, Cat # 801202, 1:1000) or for neuronal nuclei with Islet-1 (Novus Biologicals, Cat # af1837-sp, 1:500) antibodies, while YFP positive neurons were identified by endogenous GFP expression. Nuclear expression of ATF3 (Novus Biologicals, Cat # NBP1-85816, 1:250) and Jun (Cell Signaling, Cat # 9165S, 1:500) was assessed in all Islet-1 positive neuronal nuclei. NF200 positive (Abcam, Cat # ab4680, 1:1000) and TrkA negative (EMD Millipore, Cat # 06-574, 1:500) staining was used to characterize DC neurons in YFP positive neurons. For cell culture experiments in Thy1 YFP16 mice, percent axon initiation (neurons with axon length > 50um) and radial length (distance from soma to furthest axonal point) was manually measured for TUJ1 positive and YFP positive neurons. For FASN inhibition experiments, automated cell body counts and neurite tracing and length quantification was performed using Nikon elements analysis explorer software.

Whole DRG RNA sequencing

L4 DRG were dissected and homogenized in 300µl of lysis buffer on ice and RNA purified using the PureLink RNA Mini kit (Thermo Fisher), which was submitted to the Genome Technology Access Center (GTAC) at Washington University for library preparation and

sequencing. RNA quality was assessed using an Agilent Bioanalyzer (RIN > 8). Samples were subjected to DNase treatment. rRNA depletion was achieved with the Ribo-Zero rRNA removal kit. Library preparation was performed using the SMARTer kit (Clontech), and sequencing performed on an Illumina HiSeq3000.

Briefly, sequences are adapter-trimmed using Cutadapt (Martin, 2011) and subjected to quality control using PRINSEQ (Schmieder & Edwards, 2011) and aligned to mouse genome GRCm38/mm10 using STAR (Dobin et al., 2013). Sequencing performance was assessed for total number of aligned reads, total number of uniquely aligned reads, genes and transcripts detected, ribosomal fraction, known junction saturation, and reads distribution over known gene models with RSeQC (L. Wang, Wang, & Li, 2012). Reads in features were counted using HTseq (Anders, Pyl, & Huber, 2015). Genes differentially expressed between conditions were identified using DESeq2 with a false discovery rate (FDR) adjusted p values < 0.1 (Love, Huber, & Anders, 2014). Variance stabilizing transformation (VST) normalized counts were calculated using DESeq2, and normalized gene counts were converted to Z scores for plotting. Heatmaps were generated using heatmap.2 function of the gplots R package.

Fluorescence-Activated Cell Sorting RNA Sequencing (FACS-seq)

L4 DRG from Thy1-YFP16 mice were dissociated as described above and FACS-sorted as previously described (Carlin et al., 2019). Briefly, after dissociation cells were passed through a 70um cell strainer and resuspended in PBS with 2% fetal calf serum. L4 DRG cells were sorted by GFP signal in triplicate for each sample (100 cells per well) and sent to GTAC for library preparation and sequencing. Library preparation was performed using the SMARTer Ultra LowRNA kit (Clontech) and sequencing performed on an Illumina HiSeq3000. Differentially expressed gene analysis were performed as described above except noted below. Genes with < 20 reads in all samples were excluded from further analysis. Outlier samples were identified using robust principal component analysis according to the ROBPCA, and GRID algorithms

implemented in rrcov R package and were removed from further analysis. The factors of unwanted variation were estimated using RUVr with k = 2 and were modeled in the DESeq2 design formula (Risso, Ngai, Speed, & Dudoit, 2014).

Data Deposition

FASTQ files were deposited at the NCBI GEO database. Accession: GSE149646

Statistical Analysis

All quantifications used for statistical analysis was performed by experimenters blinded to treatment conditions. DESeq2 with a false discovery rate (FDR) adjusted p values < 0.1. GraphPad Prism software was used for statistical analysis. Statistical tests, sample sizes, and p-values are reported in the legend for each figure. Statistical significance was defined as $p < 0.05$ or adjusted $p < 0.1$ for RNA-seq experiments. Error bars indicate the standard error of the mean (SEM).

Acknowledgments

We would like to thank members of the Cavalli lab for valuable discussions. We also thank Anushree Seth and Madison Mack in association with InPrint for illustration in Fig.2a. This work was funded in part by a post-doctoral fellowship from the Craig H. Neilsen Foundation to E.E.E, by NIH grant NS096034, NS082446 and R21EY029077 to V.C.

Competing interest

The authors declare no competing interests.

Figure 1 with 1 supplement

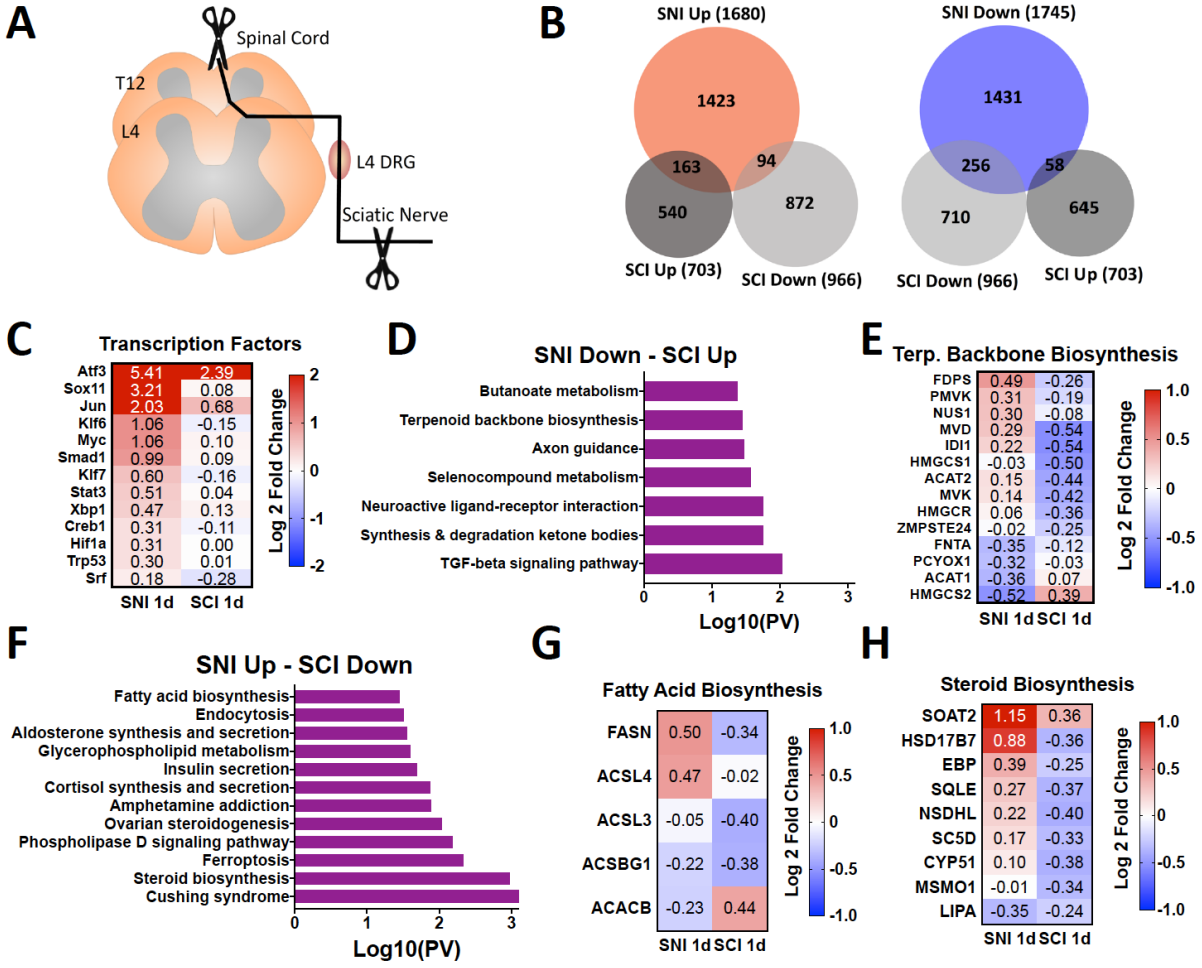

Spinal Cord Injury (SCI) induces an acute transcriptional response in the dorsal root ganglion (DRG) that differs from sciatic nerve injury (SNI).

A) Schematic of the experimental design for L4 DRG RNA sequencing after SNI (n=3) and SCI (n=4). **B)** Proportional Venn diagrams for differentially expressed (DE) genes upregulated (red) or downregulated (blue) after SNI and SCI (p-adj < 0.1). **C**) Heatmap of known regeneration-associated transcription factors (RATF's) after SNI and SCI. **D**) Pathway analysis of DE genes downregulated after SNI and upregulated after SCI (KEGG 2016). **E**) Heatmap of genes associated with terpenoid backbone biosynthesis after SNI and SCI. **F**) Pathway analysis of DE

genes upregulated after SNI and downregulated after SCI (KEGG 2016**). G-H**) Heatmap of genes associated with fatty acid biosynthesis and steroid biosynthesis after SNI and SCI.

Figure 1 – figure supplement 1

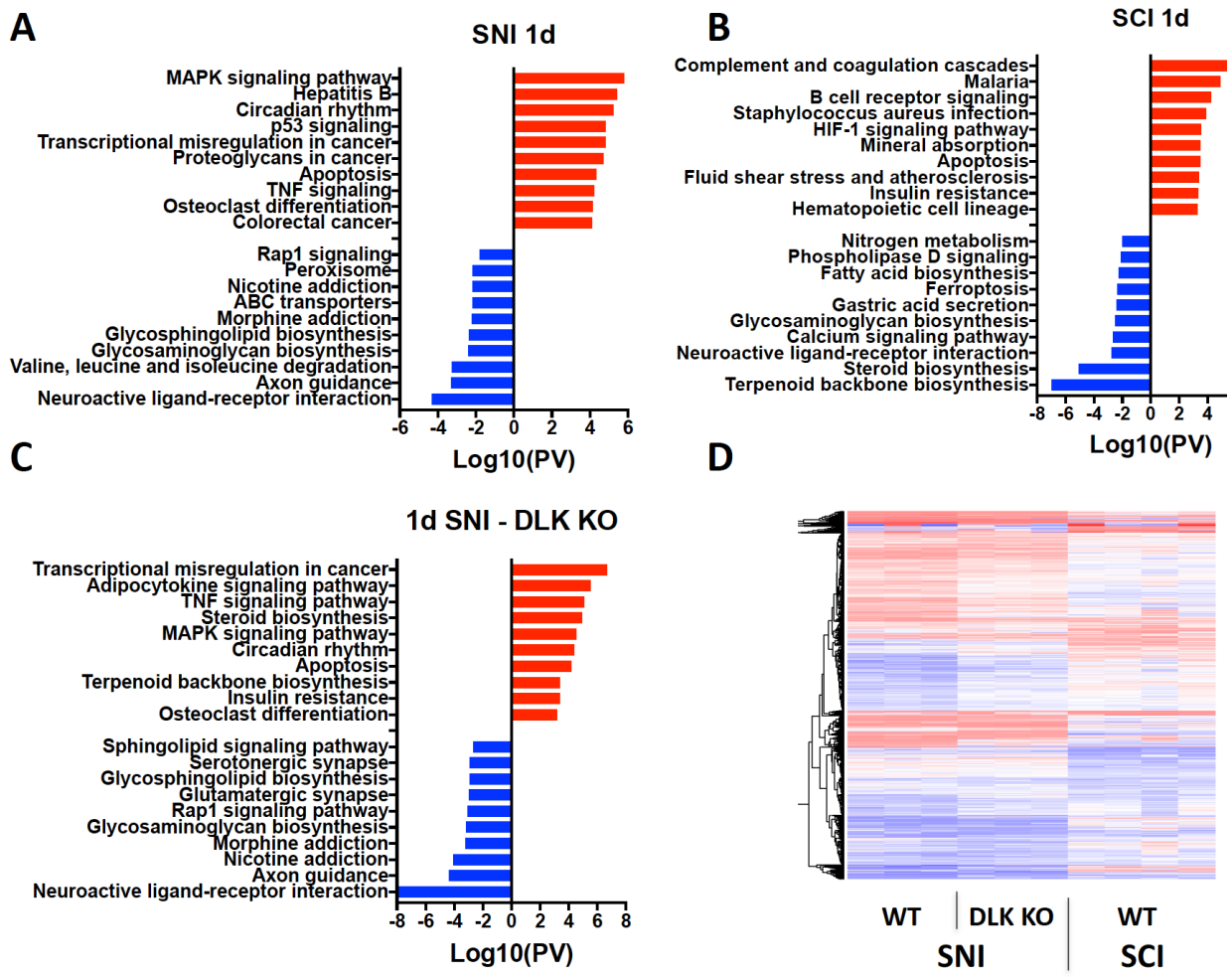

Pathway analysis and transcriptional comparison after sciatic nerve injury (SNI) and spinal cord injury (SCI) in dorsal root ganglion (DRG).

A-C) Pathway analysis for the most significantly enriched pathways associated with upregulated (red) and downregulated (blue) differentially expressed (DE) genes after SNI (n=3) or SCI (n=4) in wildtype or SNI in dual leucine zipper kinase (DLK) knockout mice (n=3; p-adj < 0.1; KEGG 2016). **D**) Heatmap of all upregulated (red) and downregulated (blue) DE genes for each subject and each condition.

Figure 2 with 1 supplement

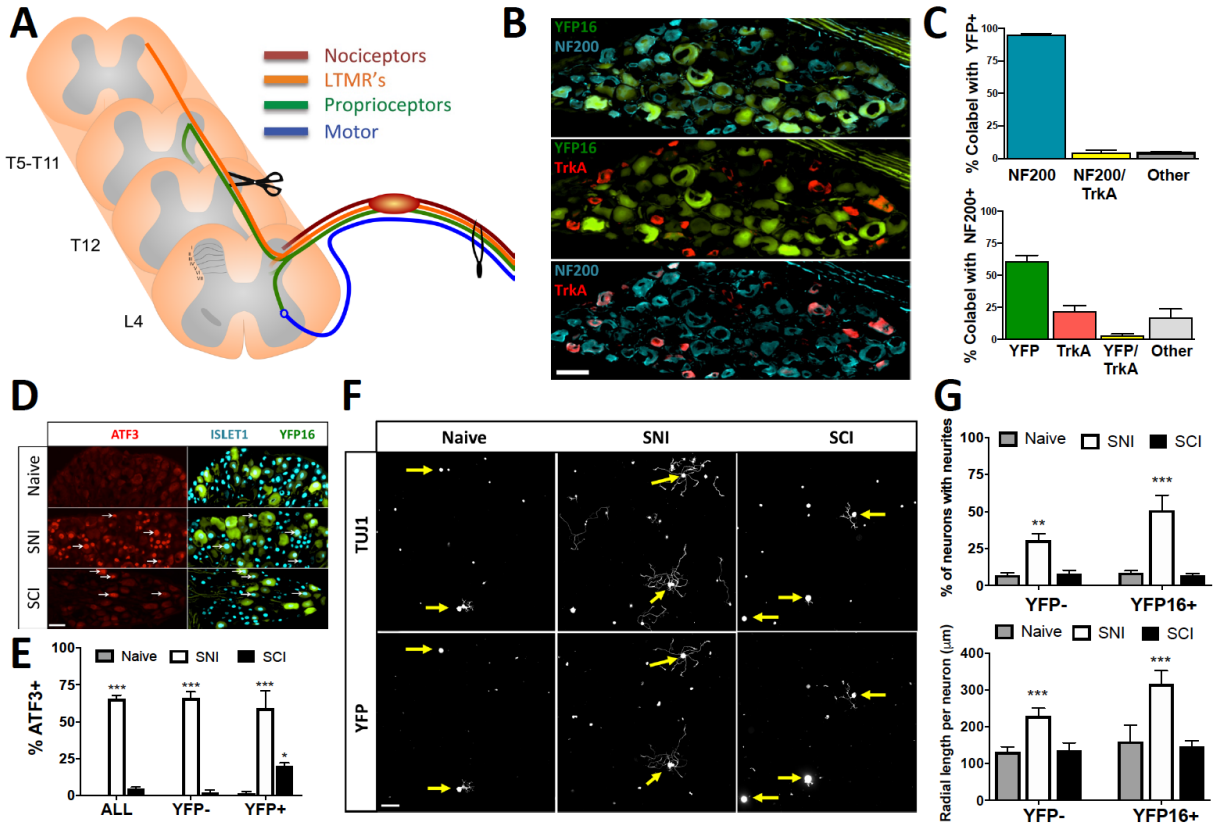

Spinal Cord Injury (SCI) does not induce a pro-growth state in dorsal column (DC) neurons *in vitro*.

A) Schematic of the experimental design and peripheral and central projects of major sensory neuron subtypes of L4 dorsal root ganglion (DRG) neurons. **B**) Representative images of L4 dorsal root ganglion (DRG) neurons from Thy1YFP16 mice labeled with NF200 (blue) and TrkA (red) antibodies. **C**) Quantification of **B** indicating percent overlap of YFP, NF200, and TrkA labeling in Thy1YFP16 mice (n=4). **D**) Representative images of L4 DRG neurons labeled with ATF3 and Islet1 antibodies in Thy1YFP16 mice in naive or 3 days after sciatic nerve injury (SNI) or SCI. **E**) Quantification of **D** indicating percentage of ATF3 positive, Islet-1 labeled neuronal nuclei in all neurons, as well as YFP negative and YFP positive neurons, for each condition (n=3/group; 2-way ANOVA). White arrowheads point to ATF3 positive neuronal nuclei. **F**) Representative images of cultured cells from L4 DRG labeled for all neurons (TUJ1) and YFP

positive neurons in naïve or 3 days after SNI or SCI. **G**) Quantification of **F** indicating the percentage of neurons extending neurites and the average radial length of neurites, in YFP negative and YFP positive neurons, for each condition (n=4/group; 2-way ANOVA). Yellow arrows point to the cell body of YFP positive neurons. *p < 0.05, **p < 0.01, ***p < 0.001

Figure 2 – figure supplement 2

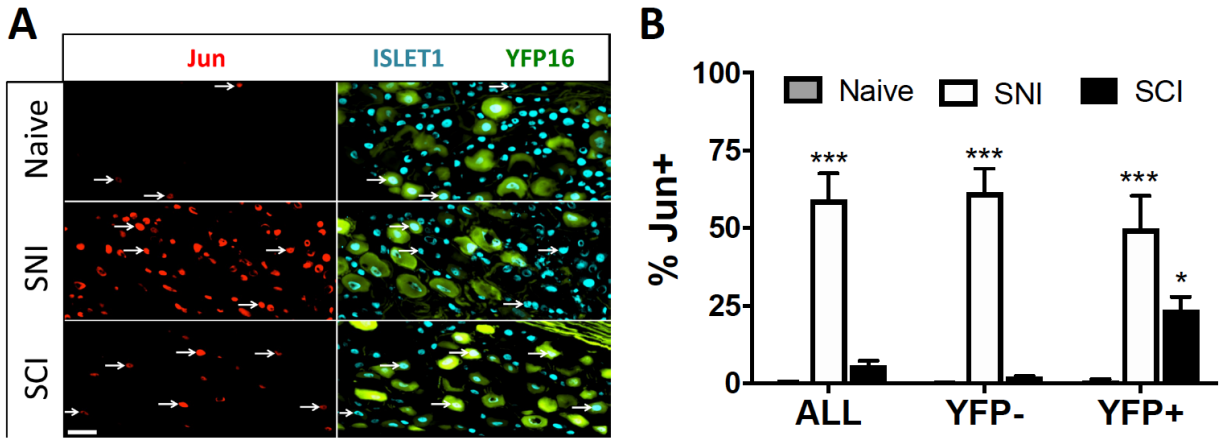

Jun upregulation is specific to dorsal column (DC) neurons after spinal cord injury (SCI). **A**) Representative images of L4 dorsal root ganglion (DRG) neurons labeled with Jun and Islet1 antibodies in Thy1YFP16 mice in naive or 3 days after sciatic nerve injury (SNI) or SCI. **B**) Quantification of **A** indicating percentage of Jun positive, Islet-1 labeled neuronal nuclei in all neurons, as well as YFP negative and YFP positive neurons, for each condition (n=3/group; 2-way ANOVA). White arrowheads point to Jun positive neuronal nuclei. *$p < 0.05$, ***$p < 0.001$

Figure 3 with 1 supplement

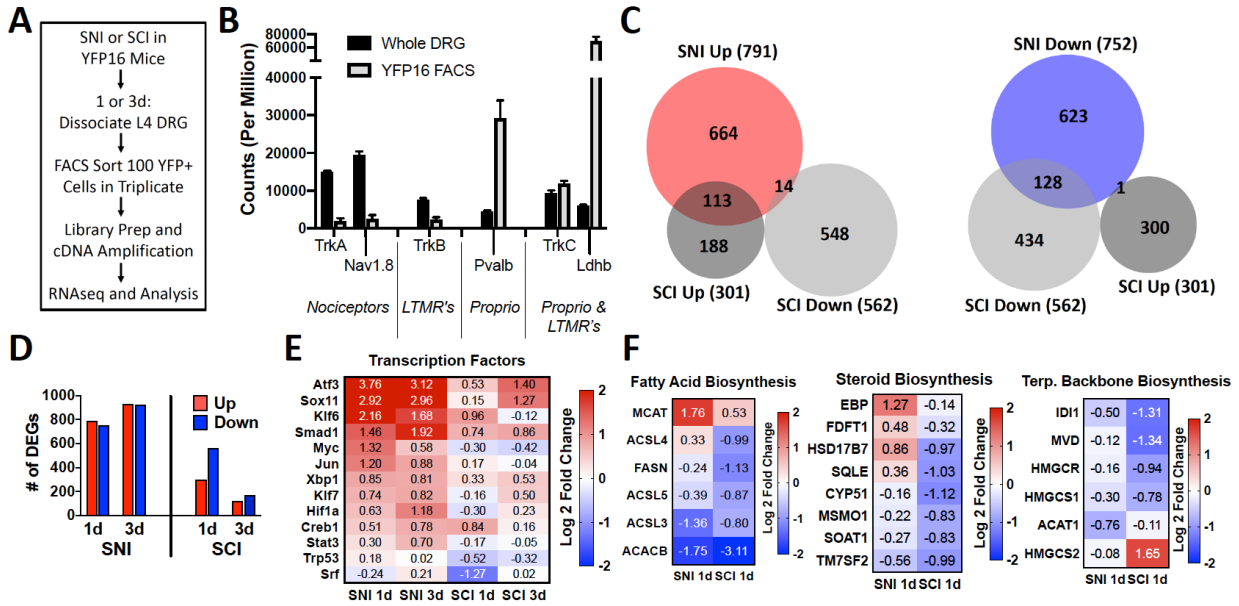

Spinal Cord Injury (SCI) induces an acute transcriptional response in dorsal column (DC) neurons that mostly differs from sciatic nerve injury (SNI).

A) Schematic of the experimental design for fluorescence-activated cell sorting (FACS) of DC neurons from Thy1YFP16 mice 1 or 3 days after SNI or SCI (n=3 per group, except n=4 for naïve and SCI 1d). **B**) Total counts of genes associated with three predominant neuronal subtypes in the DRG (nociceptors, low-threshold mechanoreceptors (LTMR's), and proprioceptors (Proprio)). **C**) Proportional venn diagrams for differentially expressed (DE) genes upregulated (red) or downregulated (blue) 1 day after SNI and SCI in DC neurons, and **D**) Number of DE genes 1 and 3 days after SNI or SCI (p-adj < 0.1, RUvR = 2). **E**) Heatmap of known regeneration-associated transcription factors (RATF's) 1 and 3 days after SNI and SCI in DC neurons. **F**) Heatmap of genes associated with fatty acid biosynthesis, steroid biosynthesis, and terpenoid backbone biosynthesis 1 day after SNI and SCI in DC neurons.

Figure 3 – figure supplement 3

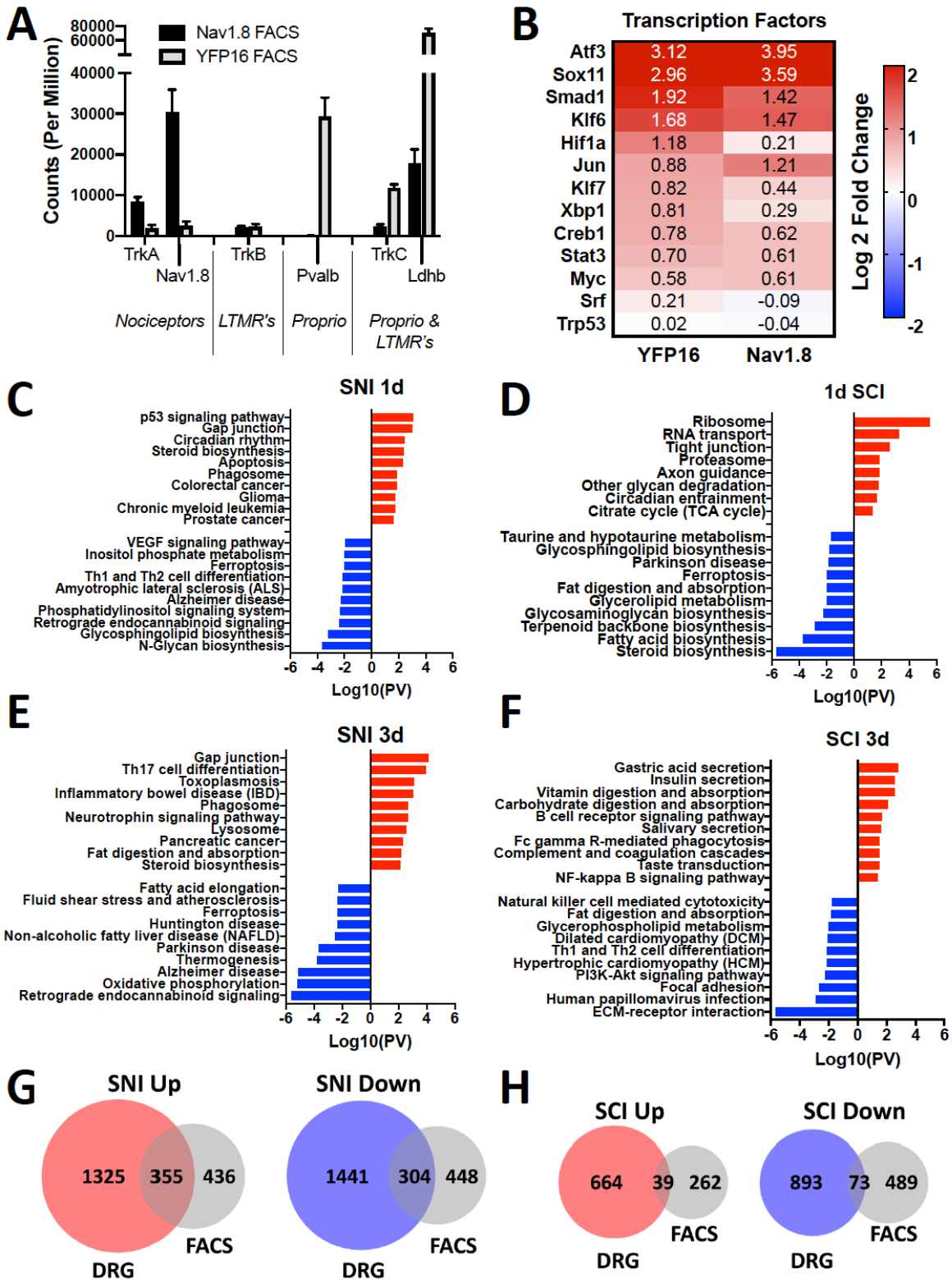

Pathway analysis and transcriptional response of DC neurons 1 and 3 days after sciatic nerve injury (SNI) and spinal cord injury (SCI).

A) Comparison of total counts of genes associated with three predominant neuronal subtypes in the DRG (nociceptors, low-threshold mechanoreceptors (LTMR's), and proprioceptors (Proprio)) between fluorescence-activated cell sorted (FACS) nociceptors (Nav1.8) and DC neurons (Thy1YFP16). **B**) Heatmap of known regeneration-associated transcription factors (RATF's) 3 days after SNI in FACS sorted nociceptors (Nav1.8) and DC neurons (Thy1YFP16). **C-F**) Pathway analysis for the most significantly enriched pathways associated with upregulated (red) and downregulated (blue) differentially expressed (DE) genes 1 and 3 days after SNI (n=3) or SCI (n=4 (1d), n=3 (3d)) in DC neurons (KEGG 2016). **G-H**) Proportional venn diagrams for DE genes upregulated (red) or downregulated (blue) 1 day after SNI and SCI in whole DRG (p-adj<0.1) compared with DC neurons (p-adj<0.1, RUvR = 2).

Figure 4

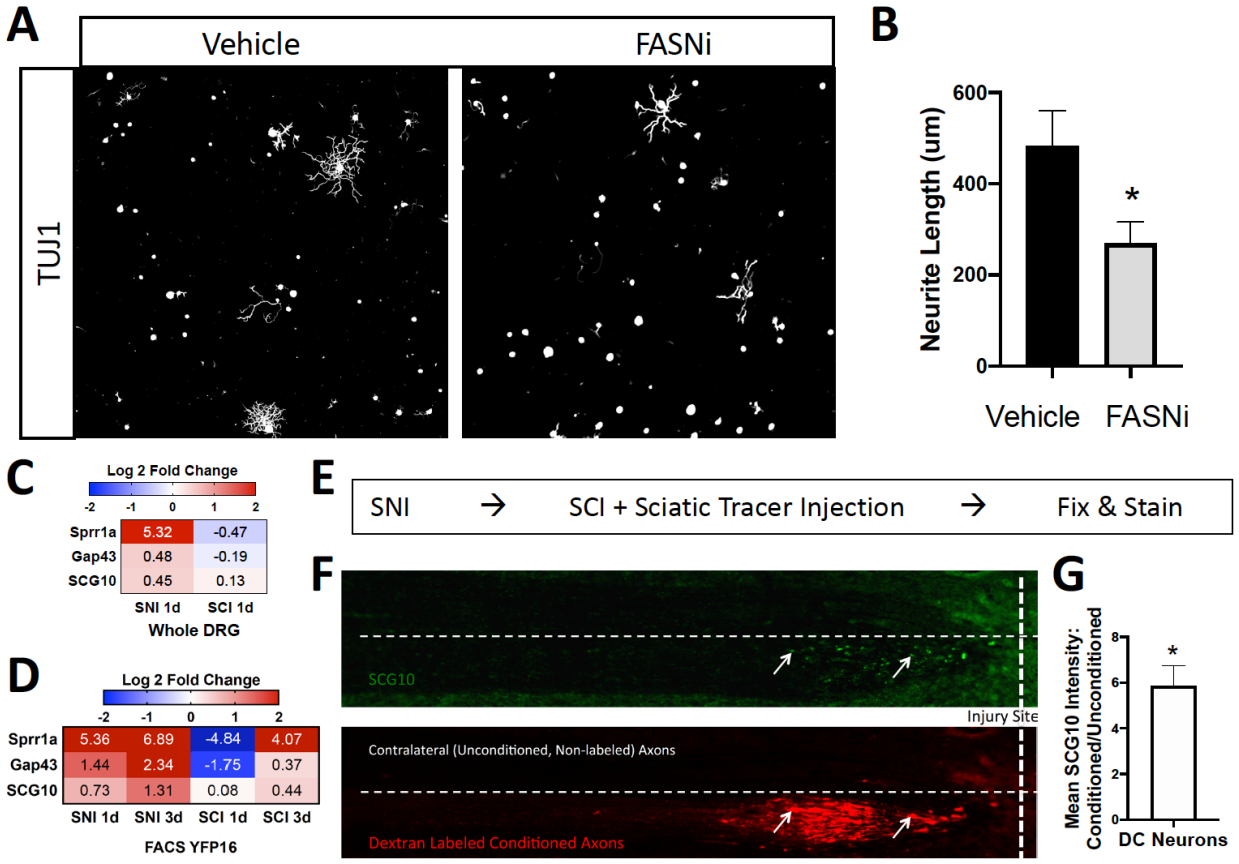

Fasn inhibition decreases sensory neuron growth *in vitro*.

A) Representative images of TUJ1-labeled sensory neurons cultured from L4 dorsal root ganglion (DRG), that were treated with vehicle or 1um of platensimycin 1 hour after plating, and then allowed to grow for 24hr in culture. **B**) Quantification of **A** indicating the average neurite length for each neuron for each condition; automated neurite tracing and length quantifications were performed using Nikon Elements software (n=4/condition; Unpaired t-test). **C,D**) Heatmap of genes for known axonally-trafficked protein genes 1 and 3 days after SNI and SCI in whole DRG or fluorescence-activated cell sorted (FACS) dorsal column (DC) neurons from Thy1YFP16 mice. **E**) Schematic indicating the experimental design for the *in vivo* conditioning experiment. **F**) Representative images of horizontal sections of the dorsal column labeled with SCG10 and dextran-labeled conditioned axons that was injected into the ipsilateral sciatic nerve. **G**)

Quantification of **F** indicating the ratio of mean SCG10 staining intensity between conditioned and unconditioned axons of DC neurons (One-sample t-test and Wilcoxon signed rank test). *p < 0.05

References

Abe, N., & Cavalli, V. (2008). Nerve injury signaling. *Curr Opin Neurobiol*.

Anders, S., Pyl, P. T., & Huber, W. (2015). HTSeq--a Python framework to work with high-throughput sequencing data. *Bioinformatics, 31*(2), 166-169. doi:10.1093/bioinformatics/btu638

Blackmore, M. G. (2012). Molecular control of axon growth: insights from comparative gene profiling and high-throughput screening. *Int Rev Neurobiol, 105*, 39-70. doi:B978-0-12-398309-1.00004-4 [pii]
10.1016/B978-0-12-398309-1.00004-4

Blackmore, M. G., Wang, Z., Lerch, J. K., Motti, D., Zhang, Y. P., Shields, C. B., . . . Bixby, J. L. (2012). Kruppel-like Factor 7 engineered for transcriptional activation promotes axon regeneration in the adult corticospinal tract. *Proc Natl Acad Sci U S A, 109*(19), 7517-7522. doi:10.1073/pnas.1120684109

Carlin, D., Halevi, A. E., Ewan, E. E., Moore, A. M., & Cavalli, V. (2019). Nociceptor Deletion of Tsc2 Enhances Axon Regeneration by Inducing a Conditioning Injury Response in Dorsal Root Ganglia. *eNeuro, 6*(3). doi:10.1523/ENEURO.0168-19.2019

Chandran, V., Coppola, G., Nawabi, H., Omura, T., Versano, R., Huebner, E. A., . . . Geschwind, D. H. (2016). A Systems-Level Analysis of the Peripheral Nerve Intrinsic Axonal Growth Program. *Neuron, 89*(5), 956-970. doi:10.1016/j.neuron.2016.01.034

Dean, J. M., & Lodhi, I. J. (2018). Structural and functional roles of ether lipids. *Protein Cell, 9*(2), 196-206. doi:10.1007/s13238-017-0423-5

Di Maio, A., Skuba, A., Himes, B. T., Bhagat, S. L., Hyun, J. K., Tessler, A., . . . Son, Y. J. (2011). In vivo imaging of dorsal root regeneration: rapid immobilization and presynaptic differentiation at the CNS/PNS border. *J Neurosci, 31*(12), 4569-4582. doi:10.1523/JNEUROSCI.4638-10.2011

Di Paolo, G., Lutjens, R., Pellier, V., Stimpson, S. A., Beuchat, M. H., Catsicas, S., & Grenningloh, G. (1997). Targeting of SCG10 to the area of the Golgi complex is mediated by its NH2-terminal region. *J Biol Chem, 272*(8), 5175-5182. doi:10.1074/jbc.272.8.5175

Dobin, A., Davis, C. A., Schlesinger, F., Drenkow, J., Zaleski, C., Jha, S., . . . Gingeras, T. R. (2013). STAR: ultrafast universal RNA-seq aligner. *Bioinformatics, 29*(1), 15-21. doi:10.1093/bioinformatics/bts635

Enes, J., Langwieser, N., Ruschel, J., Carballosa-Gonzalez, M. M., Klug, A., Traut, M. H., . . . Bradke, F. (2010). Electrical activity suppresses axon growth through Ca(v)1.2 channels in adult primary sensory neurons. *Curr Biol, 20*(13), 1154-1164. doi:10.1016/j.cub.2010.05.055

Fagoe, N. D., Attwell, C. L., Kouwenhoven, D., Verhaagen, J., & Mason, M. R. (2015). Overexpression of ATF3 or the combination of ATF3, c-Jun, STAT3 and Smad1 promotes regeneration of the central axon branch of sensory neurons but without synergistic effects. *Hum Mol Genet, 24*(23), 6788-6800. doi:10.1093/hmg/ddv383

Fagoe, N. D., van Heest, J., & Verhaagen, J. (2014). Spinal cord injury and the neuron-intrinsic regeneration-associated gene program. *Neuromolecular Med, 16*(4), 799-813. doi:10.1007/s12017-014-8329-3

Feng, G., Mellor, R. H., Bernstein, M., Keller-Peck, C., Nguyen, Q. T., Wallace, M., . . . Sanes, J. R. (2000). Imaging neuronal subsets in transgenic mice expressing multiple spectral variants of GFP. *Neuron, 28*(1), 41-51.

Gao, Y., Deng, K., Hou, J., Bryson, J. B., Barco, A., Nikulina, E., . . . Filbin, M. T. (2004). Activated CREB is sufficient to overcome inhibitors in myelin and promote spinal axon regeneration in vivo. *Neuron, 44*(4), 609-621. doi:10.1016/j.neuron.2004.10.030

He, M., Ding, Y., Chu, C., Tang, J., Xiao, Q., & Luo, Z. G. (2016). Autophagy induction stabilizes microtubules and promotes axon regeneration after spinal cord injury. *Proc Natl Acad Sci U S A, 113*(40), 11324-11329. doi:10.1073/pnas.1611282113

Holland, S. M., & Thomas, G. M. (2017). Roles of palmitoylation in axon growth, degeneration and regeneration. *J Neurosci Res, 95*(8), 1528-1539. doi:10.1002/jnr.24003

Jones, L. L., Margolis, R. U., & Tuszynski, M. H. (2003). The chondroitin sulfate proteoglycans neurocan, brevican, phosphacan, and versican are differentially regulated following spinal cord injury. *Exp Neurol, 182*(2), 399-411. doi:10.1016/s0014-4886(03)00087-6

Kadoya, K., Tsukada, S., Lu, P., Coppola, G., Geschwind, D., Filbin, M. T., . . . Tuszynski, M. H. (2009). Combined intrinsic and extrinsic neuronal mechanisms facilitate bridging axonal regeneration one year after spinal cord injury. *Neuron, 64*(2), 165-172. doi:10.1016/j.neuron.2009.09.016

Koseki, H., Donega, M., Lam, B. Y., Petrova, V., van Erp, S., Yeo, G. S., . . . Fawcett, J. W. (2017). Selective Rab11 transport and the intrinsic regenerative ability of CNS axons. *Elife, 6*. doi:10.7554/eLife.26956

Loh, Y. E., Koemeter-Cox, A., Finelli, M. J., Shen, L., Friedel, R. H., & Zou, H. (2017). Comprehensive mapping of 5-hydroxymethylcytosine epigenetic dynamics in axon regeneration. *Epigenetics, 12*(2), 77-92. doi:10.1080/15592294.2016.1264560

Love, M. I., Huber, W., & Anders, S. (2014). Moderated estimation of fold change and dispersion for RNA-seq data with DESeq2. *Genome Biol, 15*(12), 550. doi:10.1186/s13059-014-0550-8

Lutjens, R., Igarashi, M., Pellier, V., Blasey, H., Di Paolo, G., Ruchti, E., . . . Grenningloh, G. (2000). Localization and targeting of SCG10 to the trans-Golgi apparatus and growth cone vesicles. *Eur J Neurosci, 12*(7), 2224-2234. doi:10.1046/j.1460-9568.2000.00112.x

Mahar, M., & Cavalli, V. (2018). Intrinsic mechanisms of neuronal axon regeneration. *Nat Rev Neurosci, 19*(6), 323-337. doi:10.1038/s41583-018-0001-8

Mar, F. M., Simoes, A. R., Leite, S., Morgado, M. M., Santos, T. E., Rodrigo, I. S., . . . Sousa, M. M. (2014). CNS axons globally increase axonal transport after peripheral conditioning. *J Neurosci, 34*(17), 5965-5970. doi:10.1523/JNEUROSCI.4680-13.2014

Martin, M. (2011). Cutadapt removes adapter sequences from high-throughput sequencing reads. *EMBnet.journal, 17*(1), 10-12. doi:https://doi.org/10.14806/ej.17.1.200

McQuarrie, I. G., & Grafstein, B. (1973). Axon outgrowth enhanced by a previous nerve injury. *Arch Neurol, 29*(1), 53-55.

Morii, H., Shiraishi-Yamaguchi, Y., & Mori, N. (2006). SCG10, a microtubule destabilizing factor, stimulates the neurite outgrowth by modulating microtubule dynamics in rat hippocampal primary cultured neurons. *J Neurobiol, 66*(10), 1101-1114. doi:10.1002/neu.20295

Nakato, M., Matsuo, M., Kono, N., Arita, M., Arai, H., Ogawa, J., . . . Ueda, K. (2015). Neurite outgrowth stimulation by n-3 and n-6 PUFAs of phospholipids in apoE-containing lipoproteins secreted from glial cells. *J Lipid Res, 56*(10), 1880-1890. doi:10.1194/jlr.M058164

Neumann, S., & Woolf, C. J. (1999). Regeneration of dorsal column fibers into and beyond the lesion site following adult spinal cord injury. *Neuron, 23*(1), 83-91.

Nguyen, M. Q., Le Pichon, C. E., & Ryba, N. (2019). Stereotyped transcriptomic transformation of somatosensory neurons in response to injury. *Elife, 8*. doi:10.7554/eLife.49679

Niu, J., Ding, L., Li, J. J., Kim, H., Liu, J., Li, H., . . . Luo, W. (2013). Modality-based organization of ascending somatosensory axons in the direct dorsal column pathway. *J Neurosci, 33*(45), 17691-17709. doi:10.1523/JNEUROSCI.3429-13.2013

Palmisano, I., Danzi, M. C., Hutson, T. H., Zhou, L., McLachlan, E., Serger, E., . . . Di Giovanni, S. (2019). Epigenomic signatures underpin the axonal regenerative ability of dorsal root ganglia sensory neurons. *Nat Neurosci*. doi:10.1038/s41593-019-0490-4

Posse de Chaves, E., Vance, D. E., Campenot, R. B., & Vance, J. E. (1995). Axonal synthesis of phosphatidylcholine is required for normal axonal growth in rat sympathetic neurons. *J Cell Biol, 128*(5), 913-918.

Raivich, G., Bohatschek, M., Da Costa, C., Iwata, O., Galiano, M., Hristova, M., . . . Behrens, A. (2004). The AP-1 transcription factor c-Jun is required for efficient axonal regeneration. *Neuron, 43*(1), 57-67. doi:10.1016/j.neuron.2004.06.005

S0896627304003575 [pii]

Richardson, P. M., & Issa, V. M. (1984). Peripheral injury enhances central regeneration of primary sensory neurones. *Nature, 309*(5971), 791-793.

Riederer, B. M., Pellier, V., Antonsson, B., Di Paolo, G., Stimpson, S. A., Lutjens, R., . . . Grenningloh, G. (1997). Regulation of microtubule dynamics by the neuronal growth-associated protein SCG10. *Proc Natl Acad Sci U S A, 94*(2), 741-745. doi:10.1073/pnas.94.2.741

Rishal, I., & Fainzilber, M. (2014). Axon-soma communication in neuronal injury. *Nat Rev Neurosci, 15*(1), 32-42. doi:nrn3609 [pii]

10.1038/nrn3609

Risso, D., Ngai, J., Speed, T. P., & Dudoit, S. (2014). Normalization of RNA-seq data using factor analysis of control genes or samples. *Nat Biotechnol, 32*(9), 896-902. doi:10.1038/nbt.2931

Schmieder, R., & Edwards, R. (2011). Quality control and preprocessing of metagenomic datasets. *Bioinformatics, 27*(6), 863-864. doi:10.1093/bioinformatics/btr026

Shin, J., Cho, Y., Beirowski, B., Milbrandt, J., Cavalli, V., & DiAntonio, A. (2012). Dual leucine zipper kinase is required for retrograde injury signaling and axonal regeneration. *Neuron, 74*(6), 1015-1022.

Shin, J. E., Geisler, S., & DiAntonio, A. (2014). Dynamic regulation of SCG10 in regenerating axons after injury. *Exp Neurol, 252*, 1-11. doi:10.1016/j.expneurol.2013.11.007

Shin, J. E., Ha, H., Kim, Y. K., Cho, Y., & DiAntonio, A. (2019). DLK regulates a distinctive transcriptional regeneration program after peripheral nerve injury. *Neurobiol Dis, 127*, 178-192. doi:10.1016/j.nbd.2019.02.001

Shirane, M., & Nakayama, K. I. (2006). Protrudin induces neurite formation by directional membrane trafficking. *Science, 314*(5800), 818-821. doi:10.1126/science.1134027

Sofroniew, M. V. (2018). Dissecting spinal cord regeneration. *Nature, 557*(7705), 343-350. doi:10.1038/s41586-018-0068-4

Taylor-Clark, T. E., Wu, K. Y., Thompson, J. A., Yang, K., Bahia, P. K., & Ajmo, J. M. (2015). Thy1.2 YFP-16 transgenic mouse labels a subset of large-diameter sensory neurons that lack TRPV1 expression. *PLoS One, 10*(3), e0119538. doi:10.1371/journal.pone.0119538

Tedeschi, A., Dupraz, S., Laskowski, C. J., Xue, J., Ulas, T., Beyer, M., . . . Bradke, F. (2016). The Calcium Channel Subunit Alpha2delta2 Suppresses Axon Regeneration in the Adult CNS. *Neuron, 92*(2), 419-434. doi:10.1016/j.neuron.2016.09.026

Tedeschi, A., & He, Z. (2010). Axon regeneration: electrical silencing is a condition for regrowth. *Curr Biol, 20*(17), R713-714. doi:S0960-9822(10)00865-1 [pii]
10.1016/j.cub.2010.07.006

Thakur, M., Crow, M., Richards, N., Davey, G. I., Levine, E., Kelleher, J. H., . . . McMahon, S. B. (2014). Defining the nociceptor transcriptome. *Front Mol Neurosci, 7*, 87. doi:10.3389/fnmol.2014.00087

Tran, A. P., Warren, P. M., & Silver, J. (2018). The Biology of Regeneration Failure and Success After Spinal Cord Injury. *Physiol Rev, 98*(2), 881-917. doi:10.1152/physrev.00017.2017

Usoskin, D., Furlan, A., Islam, S., Abdo, H., Lonnerberg, P., Lou, D., . . . Ernfors, P. (2015). Unbiased classification of sensory neuron types by large-scale single-cell RNA sequencing. *Nat Neurosci, 18*(1), 145-153. doi:10.1038/nn.3881

Vance, J. E., Campenot, R. B., & Vance, D. E. (2000). The synthesis and transport of lipids for axonal growth and nerve regeneration. *Biochim Biophys Acta, 1486*(1), 84-96.

Vance, J. E., De Chaves, E. P., Campenot, R. B., & Vance, D. E. (1995). Role of axons in membrane phospholipid synthesis in rat sympathetic neurons. *Neurobiol Aging, 16*(3), 493-498; discussion 498-499.

Vance, J. E., Pan, D., Campenot, R. B., Bussiere, M., & Vance, D. E. (1994). Evidence that the major membrane lipids, except cholesterol, are made in axons of cultured rat sympathetic neurons. *J Neurochem, 62*(1), 329-337.

Wakil, S. J., Stoops, J. K., & Joshi, V. C. (1983). Fatty acid synthesis and its regulation. *Annu Rev Biochem, 52*, 537-579. doi:10.1146/annurev.bi.52.070183.002541

Wang, L., Wang, S., & Li, W. (2012). RSeQC: quality control of RNA-seq experiments. *Bioinformatics, 28*(16), 2184-2185. doi:10.1093/bioinformatics/bts356

Wang, Z., Reynolds, A., Kirry, A., Nienhaus, C., & Blackmore, M. G. (2015). Overexpression of Sox11 promotes corticospinal tract regeneration after spinal injury while interfering with functional recovery. *J Neurosci, 35*(7), 3139-3145. doi:10.1523/JNEUROSCI.2832-14.2015

Wu, M., Singh, S. B., Wang, J., Chung, C. C., Salituro, G., Karanam, B. V., . . . Li, C. (2011). Antidiabetic and antisteatotic effects of the selective fatty acid synthase (FAS) inhibitor platensimycin in mouse models of diabetes. *Proc Natl Acad Sci U S A, 108*(13), 5378-5383. doi:10.1073/pnas.1002588108

Yang, C., Wang, X., Wang, J., Wang, X., Chen, W., Lu, N., . . . Liu, K. (2020). Rewiring Neuronal Glycerolipid Metabolism Determines the Extent of Axon Regeneration. *Neuron, 105*(2), 276-292 e275. doi:10.1016/j.neuron.2019.10.009

Yasko, J. R., Moss, I. L., & Mains, R. E. (2019). Transcriptional Profiling of Non-injured Nociceptors After Spinal Cord Injury Reveals Diverse Molecular Changes. *Front Mol Neurosci, 12*, 284. doi:10.3389/fnmol.2019.00284

Zhang, C., Lu, J., Su, H., Yang, J., & Zhou, D. (2017). Fatty acid synthase cooperates with protrudin to facilitate membrane outgrowth of cellular protrusions. *Sci Rep, 7*, 46569. doi:10.1038/srep46569